Editors' Suggestion

Zero-point motion and direct-indirect band-gap crossover in layered transition-metal dichalcogenides

Luciano Ortenzi,[1,2] Luciano Pietronero,[2,1] and Emmanuele Cappelluti[3]
[1]*Istituto dei Sistemi Complessi, CNR, 00185 Roma, Italy*
[2]*Dipartimento di Fisica, Università La Sapienza, P.le A. Moro 2, 00185 Roma, Italy*
[3]*Istituto di Struttura della Materia, CNR, Division of Ultrafast Processes in Materials (FLASHit), 34149 Trieste, Italy*

(Received 17 September 2018; revised manuscript received 16 October 2018; published 26 November 2018)

Two-dimensional transition-metal dichalcogenides MX_2 (MoS_2, WS_2, $MoSe_2$,...) are among the most promising materials for band-gap engineering. Widely studied in these compounds, by means of *ab initio* techniques, is the possibility of tuning the direct-indirect gap character by means of in-plane strain. In such kind of calculations however the lattice degrees of freedom are assumed to be classical and frozen. In this paper we investigate in details the dependence of the band-gap character (direct vs indirect) on the out-of-plane distance h between the two chalcogen planes in each MX_2 unit. Using DFT calculations, we show that the band-gap character is indeed highly sensitive on the parameter h, in monolayer as well as in bilayer and bulk compounds, permitting for instance the switching from indirect to direct gap and from indirect to direct gap in monolayer systems. This scenario is furthermore analyzed in the presence of quantum lattice fluctuation induced by the zero-point motion. On the basis of a quantum analysis, we argue that the direct-indirect band-gap transitions induced by the out-of-plane strain as well as by the in-plane strain can be regarded more as continuous crossovers rather than as real sharp transitions. The consequences on the physical observables are discussed.

DOI: 10.1103/PhysRevB.98.195313

I. INTRODUCTION

The isolation of graphene, in 2004 [1,2], has opened the doors for intensive research on two-dimensional materials, i.e., layered materials that can be grown/exfoliated to atomical thickness. Within this context, layered transition-metal dichalcogenides (TMDs) MX_2 ($M = $ Mo, W; $X = $ S, Se) appear as the most promising compounds for future technological applications. The presence of many degrees of freedom (charge, spin, valley, layer, lattice, ldots), strongly entangled with each other, provides a fruitful playground for designing devices where electronic/optical/magnetic/transport properties can be tuned in a controlled and reversible way by external conditions, e.g., magnetic/electric fields, pressure, temperature, strain [3–17]. A striking difference of these materials with respect to graphene is that semiconducting TMDs present an intrinsic band gap [18–21], more suitable thus for technological applications [22] such as flexible electronics [3,23,24], nanophotonics [25–28], (photo)catalysis [29–33], optoelectronics [34], etc.

Interestingly, not only the size of the band gap but also the character (direct/indirect) can be relatively easily controlled. In MoS_2, for instance, the band-gap energy E_g changes from 1.29 eV in the bulk compounds to 1.90 eV in the monolayer. At the same time, the band gap evolves from an indirect one for $N \geqslant 2$ (N being the number of layers) to a direct one for the monolayer compounds [21,35].

Thanks to the strong entanglement between electronic and lattice degrees of freedom, mechanical deformations (strain, pressure,...) of TMDs are among the best candidates for controlling and tuning the electronic properties. For instance, within this context, in monolayer MoS_2 density-functional-theory (DFT) calculations have predicted a change from direct to indirect for strain $\gtrsim$1–4%, both for compressive and tensile in-plane strain [36–50]. Most of the *ab initio* works in this field assume classical (and static) lattice coordinates, where the electronic bands are evaluated in the perfect crystal structure (see Fig. 1 for a sketch of the crystal structure). Most of the papers, also, focus their interest on the role of the in-plane strain, whereas the internal coordinates within a single sandwich MX_2, i.e., the "thickness" of the MX_2, characterized by the vertical distance h between the chalcogen planes, is assumed to be unchanged [37,38,43,45,46], or it is optimized upon lattice relaxation [36,41,42,44,45,47]. A couple of recent papers have on the other hand focused on the role of the vertical X-X distance [51,52]. Using first-principle calculations, they fix the in-plane lattice parameter and they investigate the change in the electronic structure under uniaxial vertical compression, which in the monolayer case is directly reflected in the chalcogen distance h. In this way they pointed out how out-of-plane compression of monolayer sample can be an efficient way for lifting the valence band edge at Γ and driving thus the system towards a direct/indirect gap transition with ΓK indirect-gap character. This is due to the high sensitivity of the band structure of TMDs on the vertical X-X distance h (Fig. 1). Such direct/indirect gap transition driven by out-of-plane compression is of course less efficient in bilayer-multilayer compounds where the most of the out-of-plane compression is employed in reducing the interlayer distance between MX_2 sheets. Note that the vertical X-X distance h was there considered as a classic (frozen) parameter, and in this perspective only reductions of h were considered, as a result of pressure.

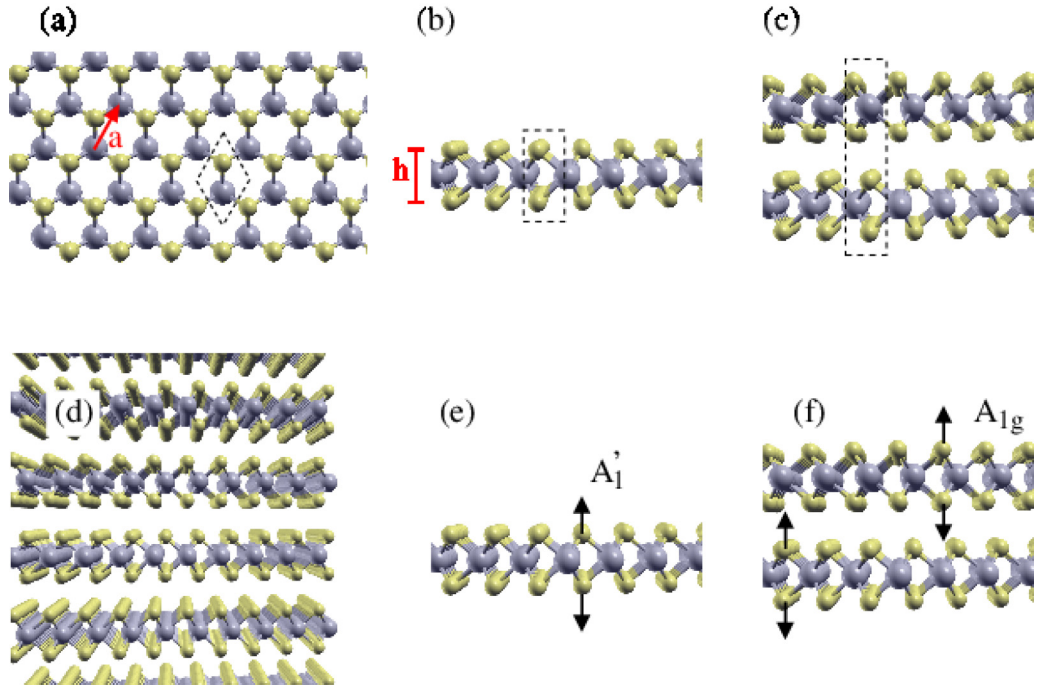

FIG. 1. (a) Top view and (b) side view of monolayer transition-metal dichalcogenides MX_2. The unit cell (marked by dashed lines) contain two X atoms and one M atom. In the top view, the bottom X atom is hidden by the top one. The structural parameters a and h are here also defined. (c) Side view of bilayer MX_2 in the 2H-MX_2 structure. The unit cell is here specified. (d) Side view of bulk MX_2 in the 2H-MX_2 structure. (e)-(f) Lattice displacements of the A_1' and A_{1g} modes in the single layer and bilayer/bulk structure, respectively.

In the present paper we show how the pointed out dependence of the electronic structure on the X-X distance h is much more relevant then in Refs. [51,52]. In particular we show how the intrinsic quantum lattice fluctuations associated with the parameter h can probe at a dynamical level a much larger range of both direct/indirect band-gap configurations than pure "classical" compression, so that the direct/indirect band-gap character cannot be captured by the analysis of the band structure of the perfect crystal (or of any "effective" band structure). In this situation the basic assumptions underlying the adiabatic Born-Oppenheimer principle are no more fulfilled and the very idea of a well-defined direct/indirect band-gap character is questionable. We show how this challenging scenario, which is more striking for monolayer compunds where a dynamical direct-gap to indirect gap can be driven, is also relevant in bilayer/multilayer compounds where a dynamical transition between two different kinds of indirect bandgap configurations, with different physical properties, can be induced.

The paper is organized as follows: In Sec. II we consider monolayer MoS_2 as textbook example to show the relevance of the zero point motion quantum lattice fluctuations and of the corresponding dynamically-induced direct/indirect-gap crossover; in Sec. III the analysis is generalized in the wider context of monolayer, bilayer, and bulk MoS_2, $MoSe_2$, WS_2, and WSe_2 investigating different kinds of indirect ($\Gamma K \leftrightarrow KQ$) band gap transitions; in Sec. IV we revise the current understanding of possible direct/indirect band-gap transitions in monolayer MoS_2 driven by in-plane strain in the light of the scenario prompted by the analysis of the lattice quantum fluctuations on strained MoS_2 monolayer; finally, in Sec. V the consequences of the above scenario are discussed.

II. DIRECT TO INDIRECT BAND-GAP CROSSOVER INDUCED BY QUANTUM FLUCTUATIONS IN SINGLE-LAYER MoS_2

In this section we investigate the role of the interplane distance h in determining the direct/indirect character of the band structure in single-layer MoS_2, with a particular regard about the effects of quantum lattice fluctuations. This analysis in single-layer MoS_2, besides being highly interesting by itself, will be used as a template to introduce the relevant concepts for the further investigation of generic transition-metal dichalcogenides MX_2 ($M = Mo$, W; $X = S$, Se).

A. Frozen phonon calculations

In the following, unless specified, we employ DFT calculations using the generalized gradient approximation (GGA) with the linear augmented plane wave (LAPW) method as implemented in the WIEN2 code [53,54]. Up to 1300 **k** points were used in the self-consistent calculations with an LAPW basis defined by the cutoff $R_S K_{\max} = 9$. The lattice parameters for bulk MoS_2 were taken from Ref. [55] (i.e., the in-plane lattice constant $a = 3.197$ Å), and single layer MoS_2 was simulated by increasing the spacing c' between layers until effective decoupling is achieved. The value of the interplane S-S distance h was taken initially to be the experimental one, $h_{\text{exp}} = 3.172$ Å.

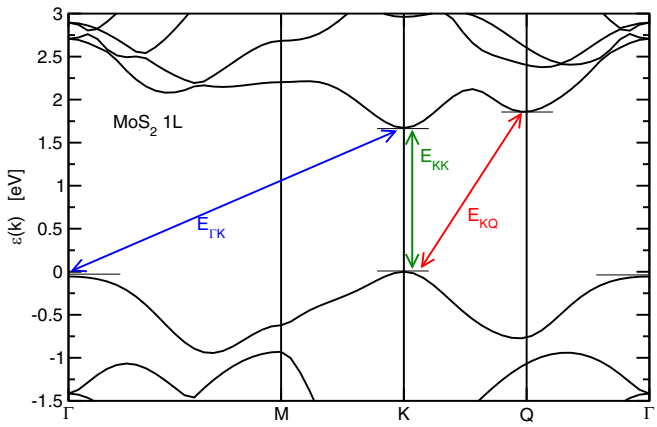

FIG. 2. Characteristic band structure of monolayer MoS_2, here evaluated within GGA calculations, with $a = 3.197$ Å and $h_{\rm exp} = 3.172$ Å. The electronic dispersion is characterized by three gaps: the direct one $E_{\rm KK}$ at the K point, the indirect one $E_{\Gamma\rm K}$ between the band edge of the valence band at the Γ point and the band edge of the conduction band at the K point, and the indirect one $E_{\rm KQ}$ between the band edge of the valence band at the K point and the band edge of the conduction band at the Q point.

The band structure of single-layer MoS_2 crystal, using these lattice parameters as representative, has been reported in uncountable papers, and it is established to have a direct gap $E_{\rm KK}$ at the K point of the Brillouin zone, as shown in Fig. 2. A secondary minimum in the conduction band is also present close to the Q point (halfway between K and Γ) with an energy difference $\Delta E_c(\rm Q)$ of the order of a few tenths of meV. The valence band is also characterized by a secondary maximum at the Γ point, with a slightly lower energy $\Delta E_v(\Gamma)$ than the top band at the K point. The precise evaluation of $\Delta E_c(\rm Q)$, $\Delta E_v(\Gamma)$ depends on computational details, as the use of the experimental or relaxed lattice coordinates, the DFT functional used (GGA vs LDA), the inclusion of many-body effects in a GW scheme, etc.

The high sensitivity of the relative energy differences $\Delta E_c(\rm Q)$, $\Delta E_v(\Gamma)$ on the lattice coordinates provides a powerful tool to search for a lattice-driven direct/indirect gap transition. Along this line, the actual possibility of a direct/indirect gap transition in the band structure, induced by in-plane (uniaxial or biaxial) strain, has been also extensively investigated by means of *ab initio* techniques. It is widely accepted that a direct/indirect band-gap transition can occur for biaxial strains of about 2%, driving the compounds, for tensile strain, towards an indirect gap $E_{\Gamma\rm K}$ between the Γ point of the valence band and the K point of the conduction band, and towards an indirect gap $E_{\rm KQ}$ between the K point of the valence band and the Q point of the conduction band, for compressive strain. In most of the papers, the lattice coordinates have been considered as classical (frozen) variables, in the absence of as well as in the presence of strain. In many cases, the h coordinate has been relaxed, so that an in-plane strain induces a change of the static h, according to the relative Poisson's ratio.

An important step further in this analysis is disentangling the role of the *in-plane* strain (namely, stretching/compression of the lattice parameter a) from the role of the *out-of-plane* strain (namely, stretching/compression of the structural parameter h) [51,52]. In Fig. 3(a) we show the band structure of monolayer MoS_2 along the cuts K-Q-Γ for a few representative values of the interplane parameter h at a fixed value of the in-plane lattice constant $a = 3.197$ Å. Unlike Refs. [51,52], herein we consider both tensile and compressive strain. We can see that relatively small changes in h can have drastic effects on the band structure and on the direct/indirect character of the band gap. The experimental value $h = 3.172$ Å has been marked with filled squares in Fig. 3(a) and it shows the typical direct gap at the K point widely reported in literature. With respect to this case, we find that further reduction of h, for vertical compression, would lead however to an indirect gap $E_{\Gamma\rm K}$, whereas further increase of h, for vertical tensile elongation, would result in an indirect gap $E_{\rm KQ}$. The plot of the different gaps E_α ($\alpha = \Gamma\rm K$, KK, KQ) as functions of h is shown in Fig. 3(b), pointing out, in this regime, a linear behavior of the gaps E_α with h. This allows us to estimate a transition between indirect (ΓK) to direct (KK) gap at $h_{c1} = 3.148$ Åand a transition between direct (KK) to indirect (KQ) gap at $h_{c2} = 3.244$ Å. A change of about 3% of the interplane distance h appears thus sufficient to change radically the character of the band gap from indirect (ΓK) to direct (KK) and to indirect (KQ).

The inclusion of the spin-orbit coupling would change quantitatively but not qualitatively this scenario. Spin orbit is indeed known to induce a band spin splitting which is largest at the K point of the valence band (±75 meV in MoS_2) and at the Q point of the conduction band, while it is relatively smaller for all the other band edges [56]. Inclusion of the spin-orbit coupling would thus mainly lower the KK and KQ band gaps in Fig. 3(b) of about ∼100 meV, slightly changing the crossing points h_{c1} and h_{c2}. The change in h_{c1}, h_{c2} is expected to be more sizable for WS_2 where the spin-orbit coupling is larger. As we are going to see in the next section, however, the precise determination of h_{c1} and h_{c2} is of secondary relevance since quantum lattice fluctuations can intrinsically span a large space of h. In addition, the effects of the spin-orbit coupling are expected to be even less relevant in multilayer ($N \geqslant 2$) systems, where the band splitting induced by the spin-orbit coupling is largely overcome by the concomitant splitting due to the interlayer coupling.

B. Zero point motion quantum lattice fluctuations

The high sensitivity of the band structure on the interplane distance h calls for a more precise assessment of the physical relevant range of h for real materials. In order to address this point, we show in Fig. 3(c) the total energy $V(h)$ of monolayer MoS_2 as a function of the parameter h. The different colored symbols mark the direct/indirect character of the band gap, whose band structure is shown in the panel (b). The minimum of $V(h)$ corresponds to the optimized (relaxed) interplane S-S distance, which we found as $h_{\rm cl} = 3.148$ Å, at the very verge of the transition between a direct and indirect band-gap character. Such a value $h_{\rm cl} = 3.148$ Å represents thus the vertical interplane S-S distance at the classical level, i.e., in the frozen perfect crystal structure, corresponding to a gap at a classical level $E_{\rm cl} = 1.653$ eV with direct KK character.

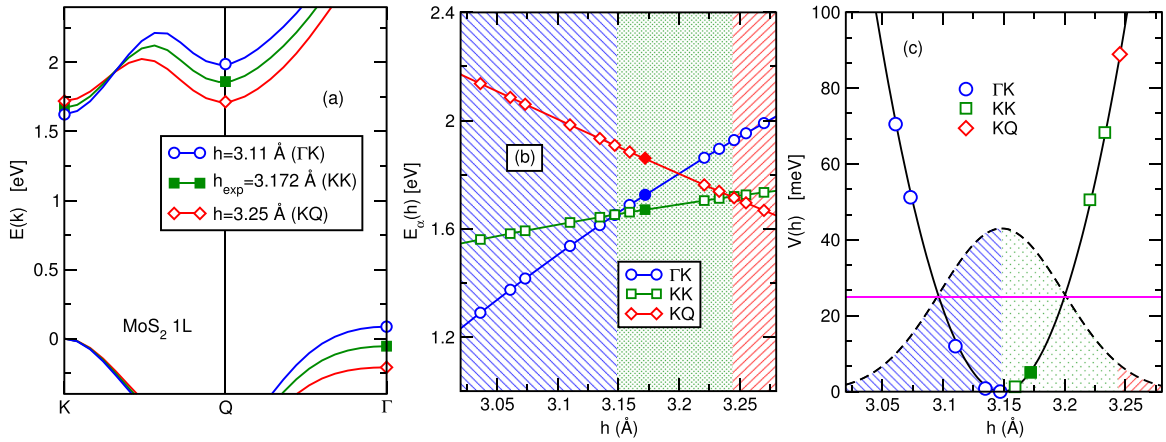

FIG. 3. Direct/indirect band-gap crossover for monolayer MoS_2 as a function of the interplane S-S structural parameter h: (a) evolution of the band structure for three representative values of h. (b) evolution of the band gaps $E_\alpha(h)$ as a function of h. An indirect gap $E_{\Gamma K}$ is predicted for $h \leqslant 3.148$ Å, a direct gap E_{KK} is predicted for $3.148\,\text{Å} \leqslant h \leqslant 3.244$ Å, and an indirect gap E_{KQ} is predicted for $h \geqslant 3.244$ Å. (c) Frozen phonon energy $V(h)$ as a function of h (open symbols). The shape and color of the symbols show the character of the gap as evaluated by panel (b). The horizontal line denotes the zero point energy $\hbar\omega_{A_1'}$, whose intercept with $V(h)$ gives the zero point motion lattice displacement. The dashed Gaussian-like line is the probability distribution $P(h)$ defined in Eq. (1), weighting the available phase space for each direct/indirect gap case.

The relevance of indirect gap states even in single layer MoS_2 appears however striking when intrinsic quantum lattice fluctuations are taken into account. To address this issue in more detail, we notice that the interplane S-S distance h is directly associated with the phonon A_1' whose lattice displacements are shown in Fig. 1(e) [57,58]. The total energy $V(h)$ reported in Fig. 3(c) can be viewed thus precisely as the frozen phonon A_1', representing the energy profile of the system as a function of the static phonon coordinate h. Quantum lattice fluctuations can be formally evaluated by fitting $V(h)$ and solving the associated quantum Schroedinger's equation for the lattice displacement [59,60]. This task can be further simplified by noticing that the frozen phonon energy potential obeys a perfect parabolic profile $V(h) = a_2(h - h_{cl})^2$, with $a_2 = 4.68\ \text{eV/Å}^2$, pointing out to the absence of anharmonic effects. The zero point motion mean square value of the quantum lattice fluctuations, h_{ZPM}, can be analytically obtained by the condition $V(h_{cl} \pm h_{ZPM}) = N_S\hbar\omega_{A_1'}/4$, as graphically shown in Fig. 3(c). Here $N_S = 2$ is the number of sulfur atoms for unit cell and $\hbar\omega_{A_1'}$ the energy of the A_1' phonon. From this simple analysis we get $h_{ZPM} = 0.051$ Å. Such an estimate is corroborated by a direct solution of the Schroedinger's equation that permits us to evaluate the ground-state wave function $\Psi_G(h)$ of the A_1' phonon and hence the probability distribution function $P(h) = |\Psi_G(h)|^2$. Given the harmonic character, $P(h)$ can be written as:

$$P(h) = \frac{1}{\sqrt{2\pi h_{ZPM}^2}} \exp\left[-\frac{(h - h_{cl})^2}{h_{ZPM}^2}\right]. \tag{1}$$

The function $P(h)$ represents the (ground-state) probability for the compound to have S-S interplane distance h. The plot of $P(h)$ is also shown in Fig. 3(c), showing that the direct band-gap character found by static *ab initio* calculations can be poorly representative of the rich phase space of this compound, where zero point motion quantum lattice fluctuations are expected to span dynamically regions with a direct gap as well as regions with an indirect gap, both with Γ-K and K-Q character.

To gain a deeper insight about this issue we can thus define, within a semiclassical framework, a probability distribution for the gap function, $P_E(E) = P[E(h)]$, where there is a one-to-one correspondence between the variable h and the band-gap value E_α with character α. In the same spirit, we can thus introduce two compact parameters, namely:

$$W_\alpha = \int_{E(h)\in E_\alpha} dE\, P_E(E), \tag{2}$$

and

$$E_\alpha = \int_{E(h)\in E_\alpha} dE\, E\, P_E(E). \tag{3}$$

The parameter W_α represents the (ground-state) probabilities to have direct or indirect gap with character $\alpha = \Gamma K$, KK, KQ, whereas E_α represents *average* band gap $\bar{E}_\alpha$ for each direct/indirect gap.

For monolayer MoS_2 we find $W_{\Gamma K} = 0.50$, $\bar{E}_{\Gamma K} = 1.502$ eV, $W_{KK} = 0.47$, $\bar{E}_{KK} = 1.671$ eV, and $W_{KQ} = 0.03$, $\bar{E}_{KQ} = 1.681$ eV. This shows that, although classical band-structure calculations with frozen lattice dynamics would predict a large direct band gap with $E_{KK} \approx 1.653$–1.670 eV (depending on the optimized or experimental value of h), quantum lattice fluctuations would suggest rather a dominance of an indirect ΓK gap with $\bar{E}_{\Gamma K} \approx 1.50$ eV, besides an additional small component with indirect KQ gap with $\bar{E}_{KQ} = 1.68$ eV.

This situation is radically unconventional compared with the physics of standard semiconductors, where the quantum lattice fluctuations do not affect at such extent the value of the band gap, nor are able to switch the direct/indirect character of the band gap. On the contrary, at a qualitative level, it appears in these compounds that electronic configurations with indirect and direct gap can be dynamically probed as

a result of quantum lattice fluctuations. In this scenario it appears thus impossible to disentangle the quantum dynamics of the lattice degrees of freedom from the electronic excitations, leading to the breakdown of the Born-Oppenheimer adiabatic assumption, which is on the base of most of the concepts of solid state physics. A rigorous theory taking into account nonadiabatic processes induced by the breakdown of the Born-Oppenheimer principle is a formidable task that is at the moment lacking in literature. In Sec. V we discuss in more detail a possible approach to tackle this scenario, compared with the relevant studies in literature, and possible physical consequences of this scenario.

III. QUANTUM LATTICE FLUCTUATIONS AND BAND GAPS IN LAYERED TRANSITION-METAL DICHALCOGENIDES

In the previous section, we have considered monolayer MoS_2 as a representative case of layered transition-metal semiconductor dichalcogenides, with a particular focus on the relevance of the interplane S-S distance h in regards to the band-gap character. This analysis has permitted us to point out a possible crossover, driven by the quantum lattice fluctuations, between direct and indirect gap. To this aim we have introduced useful quantities as the weights W_α and the average band gaps $\bar{E}_\alpha$ that describe in a synthetic way the relevance of the different electronic band structures as probed by the lattice quantum fluctuations.

The relevance of these effects is now investigated in a systematic way in the broad family of multilayer TMDs MX_2, were $M = Mo$, W and $X = S$, Se. We consider, as representative cases: monolayer compounds (1L), bilayer compounds (2L), and bulk compounds, in the conventional 2H-MX_2 stacking. Intermediate multilayer systems with $2 < N < \infty$ do not present any qualitative difference with respect to the cases $N = 2$ and bulk.

Lattice parameters in the perfect crystal structure for the bulk structure are taken from Ref. [55]. Monolayer and bilayer compounds are obtained thus by adding a vacuum region up to 10 Å between the monolayer/bilayer blocks. We employ the same computational tools as discussed in Sec. II A for monolayer MoS_2. Van der Waals interactions are thus not included. The explicit inclusion of van der Waals effects can make the harmonic probability distribution functions $P(h)$ somehow narrower, but we don't expect substantial differences in the results.

For each compound, we investigate the effects of the quantum fluctuations of the interplane X-X distance within each sandwich MX_2 [see Figs. 1(e) and 1(f)]. As mentioned, for monolayer systems this corresponds to the A_1' lattice displacement, whereas for bilayer and bulk compounds this corresponds to the A_{1g} lattice displacement [57,58]. Following what was done for monolayer MoS_2, for each compound we compute the band structure and the size of each gap $E_{\Gamma K}$, E_{KK}, E_{KQ} as functions of h. Also relevant, due to the interlayer coupling, will appear the gap ΓQ between valence states at Γ and conduction states at Q. A crucial difference between monolayer and multilayer systems with ($N \geqslant 2$) is the presence, in multilayer systems, of the interlayer coupling which split of a sizable amount the energy level at Q in the conduction band and at Γ in the valence band [35,61]. In particular, as we are going to see the interlayer splitting of the valence band edge at the Γ point is so large to prevent the possibility that changes of h, within the range of physically allowed quantum lattice fluctuations, can induce a transition of the valence band edge between the K and Γ point, as in the monolayer systems. In this perspective, unlike in the monolayer case, in multilayer systems (starting from $N = 2$) the valence band edge at Γ appears as a robust feature against quantum lattice fluctuations. On the other hand, due to the smaller content of the chalcogen p_z orbital [61], the interlayer splitting of the conduction band at the Q point is much weaker, and it does not prevent thus the h-induced transition of the conduction edge band from K to Q.

In addition to the dependence of the band structure on the parameter h, for each compound we compute also the frozen phonon energy potential $V(h)$ associated with the A_1'/A_{1g} lattice displacements. As discussed in the previous section, such joint analysis permits us to estimate the size of the lattice fluctuations associated with the zero point motion, and the weights W_α and the average band gaps $\bar{E}_\alpha$, evaluated according to Eqs. (2) and (3). The results are summarized in Fig. 4 and in Table I.

We see that the magnitude of the interplane lattice fluctuations h_{ZPM} is essentially ruled only by the atomic weight of the chalcogenide atom $X = S$, Se according to the scaling $h_{ZPM} \approx 1/\sqrt{M_X}$. In addition we note that three different band-gap characters (ΓK, KK, and KQ) can be probed in single-layer MS_2 compounds, whereas only band gaps with KK and KQ character are spanned in the relevant physical range in single-layer MSe_2.

As mentioned above, in multilayer systems, due to the interlayer coupling, a direct gap KK is not possible, but two phases with ΓK and ΓQ character (respectively, for small h and large h) are possible. A classical analysis, in our GGA calculations, would predict a well-defined ΓK character for bilayer MoS_2 and a ΓQ character for all the other structures, while both configurations are relevant at a quantum level, with different weights. Within this framework one can predict in addition that the phase ΓQ will have a stronger weight in the bulk structures than in the bilayer one. At the same time, one can expect a stronger character ΓQ in the MSe_2 compounds than in the corresponding MS_2 materials.

IV. DIRECT-INDIRECT GAP TUNING IN IN-PLANE STRAINED TMDS

In the previous section we have shown how the direct/indirect character of the band structure of monolayer MX_2 is highly sensitive to the out-of-plane interplane X-X distance h. We have also shown how the intrinsic quantum lattice fluctuations of zero point motion are expected to span different direct/indirect configurations, so that the typical direct character, predicted by *ab initio* calculations in the perfect crystal structure, should be revised and a coexistence of different direct/indirect gap characters can be induced by the lattice quantum fluctuations.

The relevance of this analysis can also be investigated in the reverse scenario, namely in systems where static DFT calculations would predict an indirect gap and where a

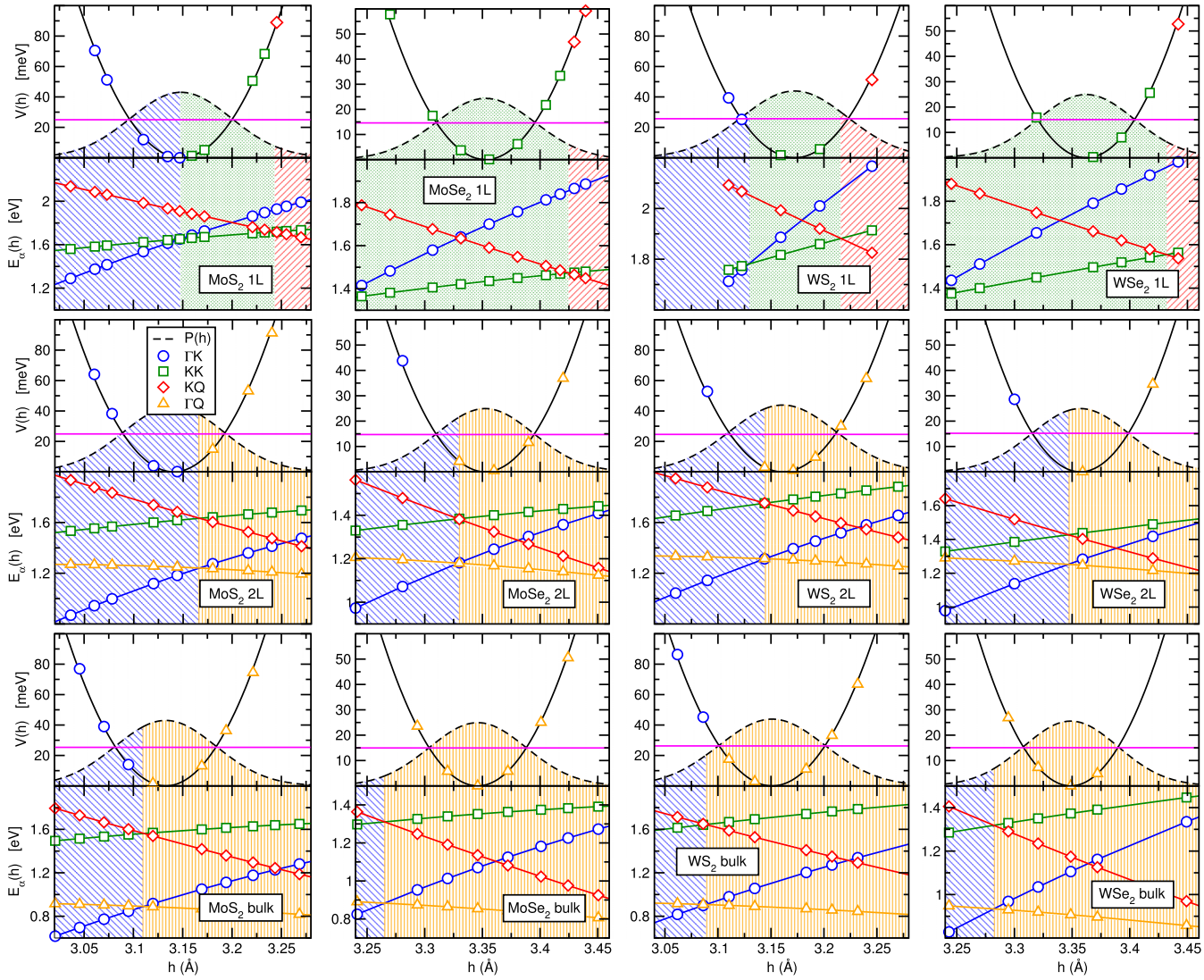

FIG. 4. Effects of the quantum lattice fluctuations on the band gap for different families of TMDs. For each compound, in the lower panel we show the evolution of the different band gaps E_α as a function of the interplane X-X distance; in the upper panel the frozen phonon DFT total energy (open symbols), the quadratic fit (solid line), the energy $\omega_{A_1'/A_{1g}}/2$ relevant for lattice quantum fluctuations (horizontal line), and the probability distribution function $P(h)$ (dashed line).

direct-gap component can be triggered in as effect of the quantum lattice fluctuations. This possibility is ruled out in bilayer and multilayer compounds where, as shown in Fig. 4 and Table I, no significant direct gap can be induced even by the zero point motion lattice quantum fluctuations. The investigation appears on the other hand interesting in monolayer TMDs under in-plane stress where, at the static lattice level, a transition from direct to indirect gap upon applying in-plane strain was discussed in many works [36–47].

To explore this scenario we consider, as a representative case, single-layer MoS_2 under biaxial in-plane uniform strain, both tensile and compressive. In Fig. 5(a) we show the phase diagram as a function of the in-plane lattice constant a, computed in our GGA calculations neglecting quantum fluctuations, i.e., using the parameter $h_{\rm cl}$ evaluated at the classical level. As shown in Sec. II in our GGA calculations (without dispersion term corrections) the unstrained case $a = 3.197$ Å corresponds to a direct KK gap situation very close to the change towards an indirect gap with ΓK character. We find thus that, at a static level, a very small tensile strain would be enough to induce a KK → ΓK transition, whereas a 1.5% of compressive strain is needed to induce a KQ gap. We stress once more that the precise determination of the phase diagram, and the location within it of the unstrained case, might depend on details of the DFT calculations. The qualitative picture is however robust and general, with a KQ gap character for compressive strain, a direct KK band structure more or less in the region of absence of in-plane strain, and a ΓK band gap in the tensile strain regime.

Such well-defined band-gap character is however questioned once intrinsic quantum lattice fluctuations are taken into account. This is shown in Figs. 5(b) and 5(c) where the band gaps $E_\alpha(h)$ and the frozen phonon energy $V(h)$ as functions of the interplane distance h are evaluated. As done in the previous sections, the effects of such zero point motion lattice fluctuations are estimated by using the probability

TABLE I. DFT evaluation of the relevant band-gap character at the classical level as well in the presence of quantum lattice fluctuations, for different families of TMDs. For each material, we report here the classical coordinate $h_{\rm cl}$, the corresponding value and character of the band gap $E_{\rm cl}$ at the classical level, the magnitude of the zero point motion lattice fluctuations $h_{\rm ZPM}$, the frequency of the relevant phonon mode, and the weight W_α and average gap $\bar{E}_\alpha$ of the relevant gaps.

		$h_{\rm cl}$ (Å)	$E_{\rm cl}$	$h_{\rm ZPM}$ (Å)	$\omega_{A_1'/A_{1g}}$ (meV)	$W_{\Gamma K}$	$\bar{E}_{\Gamma K}$ (eV)	W_{KK}	$\bar{E}_{KK}$ (eV)	W_{KQ}	$\bar{E}_{KQ}$ (eV)	$W_{\Gamma Q}$	$\bar{E}_{\Gamma Q}$ (eV)
MoS_2	(1L)	3.148	KK	0.051	50.0	0.50	1.502	0.47	1.671	0.03	1.681		
MoS_2	(2L)	3.140	ΓK	0.051	49.8	0.69	1.068					0.31	1.217
MoS_2	(bulk)	3.132	ΓQ	0.051	50.6	0.33	0.787					0.67	0.867
$MoSe_2$	(1L)	3.352	KK	0.043	29.2			0.95	1.427	0.05	1.441		
$MoSe_2$	(2L)	3.352	ΓQ	0.042	29.4	0.39	1.049					0.61	1.146
$MoSe_2$	(bulk)	3.346	ΓQ	0.042	29.9	0.03	0.855					0.97	0.851
WS_2	(1L)	3.172	KK	0.050	51.3	0.20	1.690	0.61	1.831	0.19	1.828		
WS_2	(2L)	3.161	ΓQ	0.050	50.2	0.37	1.203					0.63	1.293
WS_2	(bulk)	3.151	ΓQ	0.050	52.6	0.11	0.835					0.89	0.877
WSe_2	(1L)	3.362	KK	0.042	30.1			0.95	1.484	0.05	1.521		
WSe_2	(2L)	3.357	ΓQ	0.042	30.4	0.40	1.173					0.60	1.234
WSe_2	(bulk)	3.349	ΓQ	0.041	30.1	0.05	0.893					0.95	0.903

distribution $P(h)$ and the probability weights W_α and the corresponding averaged band gap $\bar{E}_\alpha$ are reported in Table II. For sake of comparison, we report in the same table also the probability weights W_α and the corresponding averaged band gap $\bar{E}_\alpha$ for single-layer MoS_2 without strain. From this analysis, it appears that the net direct/indirect gap transition upon strain predicted by standard *ab initio* calculation neglecting the quantum lattice fluctuations must be regarded more as a smooth continuous crossover between the relative phase spaces available for each band-gap character. Indeed, as we are going to discuss in more details, the very presence of a sizable phase space for the direct KK gap configuration can hamper the possibility of observing such crossover in photoluminescence optics. Alternative paths for observing such direct-indirect gap crossover are discussed in the next section.

V. DISCUSSION

In the previous sections, we have revised the concept of direct/indirect gap character in layered transition metal dichalcogenides MX_2, which is usually discussed in literature on the basis of a well-defined band structure, usually evaluated in first-principle calculations in the perfect crystal lattice, neglecting thus the quantum lattice dynamics. This assumption is quite justified in conventional semiconductors where there is a unique valence/conduction band edge, whose energies can be affected by the lattice dynamics but not their location in the Brillouin zone. From this perspective, the crucial novelty of TMDs is the presence of secondary band edges, both in the valence and conduction sectors, which lie only a few tenths of meV above/below the true band edges. Within this context, we have shown how a direct/indirect band-gap transition can occur as a function of the interplane distance h between the two X planes and how intrinsic zero point motion quantum lattice fluctuations of this distance can effectively span different band-gap topologies, from a direct one at K-K to indirect ones of Γ-K or K-Q character. The relevance of the different band structure probed by the lattice dynamics has thus been quantified in terms of appropriate spectral weight W_α and corresponding average band-gap energies $\bar{E}_\alpha$. On

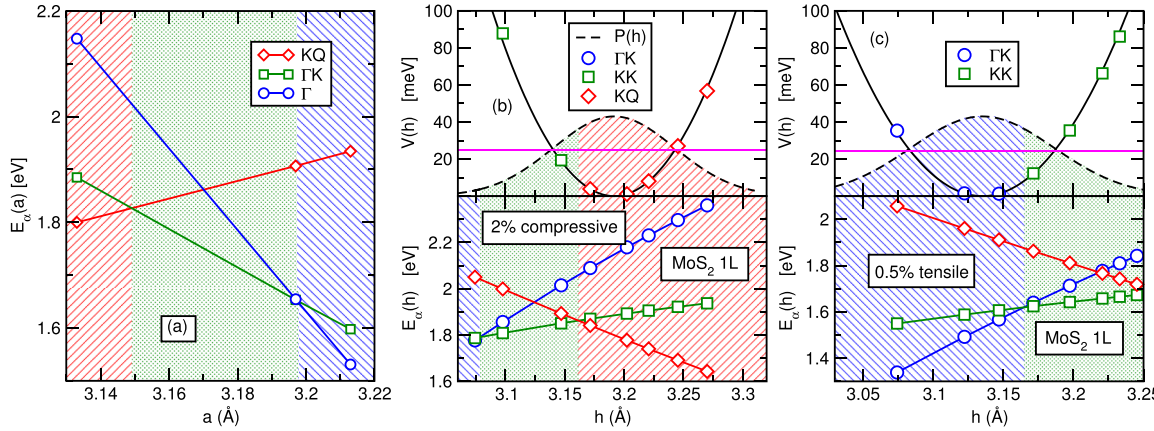

FIG. 5. (a) Band gaps E_α at the classical level (i.e., using $h_{\rm cl}$) for different in-plane lattice constants a of MoS_2 monolayer. The values of $h_{\rm cl}$ for each a are shown in Table II. (b),(c) Evolution of the band gaps E_α and of the frozen phonon energy with h for 2% compressive in-plane strain [panel (b)] and for 0.5% tensile strain [panel (c)].

TABLE II. Zero point motion h_{ZPM}, probability weights W_α, and averaged bandgap $\bar{E}_\alpha$ for single-layer MoS_2 under strain.

Single-layer MoS_2 under strain											
Strain %	a (Å)	h_{cl} (Å)	E_{cl}	h_{ZPM} (Å)	$\omega_{A_1'/A_{1g}}$ (meV)	$W_{\Gamma K}$	$\bar{E}_{\Gamma K}$ (eV)	W_{KK}	$\bar{E}_{KK}$ (eV)	W_{KQ}	$\bar{E}_{KQ}$ (eV)
−2.0	3.133	3.1916	KQ	0.051	49.8	0.01	1.748	0.27	1.837	0.72	1.753
0.0	3.197	3.1481	KK	0.051	50.0	0.50	1.502	0.47	1.671	0.03	1.681
+0.5	3.213	3.1351	ΓK	0.051	49.2	0.72	1.456	0.28	1.640		

this basis we can conclude that it is not possible to discuss electronic particle-hole excitations in terms of a well-defined direct/indirect band-gap paradigm.

A compelling analysis of the implications of these effects with respect to the physical properties observed in optics appears highly desirable, but it requires to be formally investigated in a context which goes beyond the standard Born-Oppenheimer scheme [59,60]. This is a formidable task which cannot be addressed here.

In this regard, it is worth mentioning that a promising approach, merging *ab initio* and quantum field theory calculations, has been recently developed [62–65], starting from the seminal ideas of M. Cardona [66–68], for evaluating the effects of the zero point quantum lattice fluctuations on the band structure. The basic idea of such an approach stems from a careful identification of the Feynman's diagrams associated with the zero point motion. However, although powerful, such theory is at the present mainly focused on the *single-particle* excitations, namely the one-particle Green's function and the one-particle self-energy. These quantities, evaluated in the presence of quantum lattice fluctuations, are thus used as the basic ingredients to define a renormalized effective band structure. It is interesting to stress that this approach permits us not only to define (as many other approaches) dynamically renormalized quasiparticle excitation energies but also to associate to them a *finite* lifetime/linewidth. The presence of a finite linewidth would smear the band structure (see for instance Fig. 2 in Ref. [62]) in a similar way as the dependence of the band structure on the parameter h would give a band smearing in Fig. 3(a) [59]. The *possibility* of a direct/indirect gap crossover would be detected within the context of Refs. [62–65] when the smearing of a secondary band edge is larger than the distance with the primary band edge. Note however that, in such a theory, it is not possible to investigate the coherent shift of the band edges at the Γ, K, Q points upon the lattice dynamics of the quantity h, as efficiently done in Fig. 3(a). The actual direct/indirect gap transition cannot be thus effectively assessed.

In this sense, the present analysis is complementary of the approach of Refs. [62–65], permitting us to identify the effective direct/indirect gap transition. Merging the two approaches would be highly desirable. In particular, the main challenge in this context is the prediction of observable nonadiabatic effects in the optical probes. A possible progress along this line would be the generalization of the Cardona theory to the particle-hole response function, in a conserving approach consistent with the one-particle resummation in the self-energy.

Although a compelling theory of the nonadiabatic transition between direct and indirect band-gap configurations in these materials is still lacking, few qualitative considerations about the possible effects on physical observables can at the moment be drawn. For sake of simplicity, we will consider three representative regimes: (i) a system where classical *ab initio* calculations would predict a direct gap but where quantum lattice fluctuations suggest a sizable relevance of indirect gap configurations; (ii) a system where classical *ab initio* calculations would predict an indirect gap but where quantum lattice fluctuations suggest a sizable relevance of direct gap configurations; (iii) a system where classical *ab initio* calculations would predict an indirect gap but where quantum lattice fluctuations suggest a sizable relevance of an indirect gap of a different kind.

Far from being hypothetical cases, these examples represent different possible regimes that have been so far intensively studied for theoretical and application purposes: (i) monolayer dichalcogenides MX_2 in the absence of in-plane strain; (ii) monolayer dichalcogenides MX_2 in the presence of a large enough in-plane strain inducing (at a classical level) as indirect gap band structure; (iii) multilayer dichalcogenides MX_2.

Investigating the effects of quantum lattice fluctuations in the regime (i) is probably the most crucial one, since the direct band-gap character has been claimed to be observed in many monolayer compounds (e.g., MS_2, WS_2,...) by means of photoluminescence probes. In this regard, it is worth stressing that the presence of a sizable component of an indirect-gap band structure is overall compatible and not at odds with such phenomenology since the strong intensity of the direct-gap photoemission is expected to be dominant with respect to other indirect-gap electronic configurations probed by the lattice quantum fluctuations. Similar considerations hold true for many of the optical probes related to the A and B excitons, taking into account that the band structure (and hence the optical transitions) at the K point are relatively insensitive to the lattice dynamics [see Fig. 3(a) for example]. On the other hand the spectral features associated with the exciton C are expected to be highly affected by the quantum lattice fluctuations. This might account for large broadening and for the complex structure of the C exciton as observed in optical probes [69–72]. In a similar way, traces of indirect gaps can be possibly observed in photoluminescence at different energies than the direct gap [73]. The presence of a conduction band-edge minimum at Q probed by the lattice fluctuations can have also remarkable consequences on transport properties, as explored by photoconductivity or in field-effect geometry of chemical doped systems.

Relevant effects induced by the quantum lattice fluctuations can be expected in the case (ii), representative for instance of monolayer systems under in-plane strain. Here *ab initio* calculations with frozen lattice coordinates would

classify the system as an indirect band-gap semiconductor, whereas we would predict that a sizable direct-gap band structure is dynamically probed by the quantum fluctuations. On a qualitative ground, we would expect that the presence of an even minority probability of a direct-gap configuration would be the dominant feature in a photoluminescence measurement, possibly with reduced intensity, so that photoluminescence experiments would not be able to distinguish this case from a pure direct gap case. Nevertheless, at the same time transport properties, as in case (i), are expected to be dominated by the indirect-gap character. The crossed analysis of photoluminescence and transport experiments can provide thus a route to characterize this regime. Further measurements along this line are thus encouraged.

In case (iii) the location of the valence band edge at Γ appears robust against the presence of quantum lattice fluctuations. Such quantum fluctuations however can drive a dynamical tuning between a minimum conduction band edge at K or Q. This kind of scenario is probably the most difficult to assess experimentally. Suitable ways to detect this situation rely probably in the possibility of accurate polarized optical probes where the different chiral content (and hence sensitivity to polarized light) of the minima in K and Q can be investigated. Physical consequences of this scenario can be also relevant in understanding and characterizing the observed superconducing phase in heavily electron-doped multilayered MoS_2 and other transition-metal dichalcogenides [74–80].

ACKNOWLEDGMENTS

L.O. acknowledges support from CINECA through the IsC35 TDM01 ISCRA project. E.C. acknowledges financial support from the Italian Ministero dell'Istruzione, dell'Universita' e della Ricerca-PRIN Project 2015WTW7J3.

[1] K. S. Novoselov, A. K. Geim, S. V. Morozov, D. Jiang, Y. Zhang, S. V. Dubonos, I. V. Gregorieva, and A. A. Firsov, Science **306**, 666 (2004).
[2] K. S. Novoselov, D. Jiang, F. Schedin, T. J. Booth, V. V. Khotkivich, S. V. Morozov, and A. K. Geim, Proc. Natl. Acad. Sci. **102**, 10451 (2005).
[3] B. Radisavljevic, A. Radenovic, J. Brivio, V. Giacometti, and A. Kis, Nat. Nanotech. **6**, 147 (2011).
[4] H. Zeng, J. Dai, W. Yao, D. Xiao, and X. Cui, Nat. Nanotech. **7**, 490 (2012).
[5] K. F. Mak, K. He, J. Sahn, and T. F. Heinz, Nat. Nanotech. **7**, 494 (2012).
[6] Q. H. Wang, K. Kalantar-Zadeh, A. Kis, J. N. Coleman, and M. S. Strano, Nat. Nanotech. **7**, 699 (2012).
[7] T. Cao, G. Wang, W. Han, H. Ye, C. Zhu, J. Shi, Q. Niu, P. Tan, E. Wang, B. Liu, and J. Feng, Nat. Commun. **3**, 887 (2012).
[8] H. Zeng, G.-B. Liu, J. Dai, Y. Yan, B. Zhu, R. He, L. Xie, S. Xu, X. Chen, W. Yao, and X. Cui, Sci. Rep. **3**, 1608 (2013).
[9] S. Wu, J. S. Ross, G.-B. Liu, G. Aivazian, A. Jones, Z. Fei, W. Zhu, D. Xiao, W. Yao, D. Cobden, and X. Xu, Nat. Phys. **9**, 149 (2013).
[10] Q. Wang, S. Ge, X. Li, J. Qiu, Y. Ji, J. Feng, and D. Sun, ACS Nano **7**, 11087 (2013).
[11] H. Terrones and M. Terrones, 2D Mater. **1**, 011003 (2014).
[12] X. Xu, W. Yao, D. Xiao, and T. F. Heinz, Nat. Phys. **10**, 343 (2014).
[13] R. Ganatra and Q. Zhang, ACS Nano **8**, 4074 (2014).
[14] A. Castellanos-Gomez, Nat. Phot. **10**, 202 (2016).
[15] C. Tan, X. Cao, X.-J. Wu, Q. He, J. Yang, X. Zhang, J. Chen, W. Zhao, S. Han, G.-H. Nam, M. Sindoro, and H. Zhang, Chem. Rev. **117**, 6225 (2017).
[16] R. Roldan, L. Chirolli, E. Prada, J. A. Silva-Guillen, P. San-Jose, and F. Guinea, Chem. Soc. Rev. **46**, 4387 (2017).
[17] J.-S. Kim, R. Ahmad, T. Pandey, A. Rai, S. Feng, J. Yang, Z. Lin, M. Terrones, S. K. Banerjee, A. Singh, D. Akinwande, and J.-F. Lin, 2D Mater. **5**, 015008 (2018).
[18] R. A. Bromley, R. B. Murray, and A. D. Yoffe, J. Phys. C.: Solid State Phys. **5**, 759 (1972).
[19] L. F. Mattheiss, Phys. Rev. B **8**, 3719 (1973).
[20] S. Lebègue and O. Eriksson, Phys. Rev. B **79**, 115409 (2009).
[21] K. F. Mak, C. Lee, J. Hone, J. Shan, and T. F. Heinz, Phys. Rev. Lett. **105**, 136805 (2010).
[22] L. M. Xie, Nanoscale **7**, 18392 (2015); Y. Liu, N. O. Weiss, X. D. Duan, H.-C. Cheng, Y. Huang, and X. F. Duan, Nat. Rev. Mat. **1**, 16042 (2016); A. Rai, H. C. P. Movva, A. Roy, D. Taneja, S. Chowdhury, and S. K. Banerjee, Crystals **8**, 316 (2018).
[23] For a review see for instance: G. Fioril, F. Bonaccorso, G. Iannaccone, T. Palacios, D. Neumaier, A. Seabaugh, S. K. Banerjee, and L. Colombo, Nat. Nanotech. **9**, 768 (2014), and references therein.
[24] S. B. Desai, S. R. Madhvapathy, A. B. Sachid, J. P. Llinas, Q. X. Wang, G. H. Ahn, G. Pitner, M. J. Kim, J. Bokor, C. M. Hu *et al.*, Science **354**, 99 (2016).
[25] D.-S. Tsai, K.-K. Liu, D.-H. Lien, M.-L. Tsai, C.-F. Kang, C.-A. Lin, L.-J. Li, and J.-H. He, ACS Nano **7**, 3905 (2013).
[26] O. Lopez-Sanchez, D. Lembke, M. Kayci, A. Radenovic, and A. Kis, Nat. Nanotech. **8**, 497 (2013).
[27] For a review see for instance: F. H. L. Koppens, T. Mueller, Ph. Avouris, A. C. Ferrari, M. S. Vitiello, and M. Polini, Nat. Nanotech. **9**, 780 (2014), and references therein.
[28] A. Krasnok, S. Lepeshov, and A. Alu, Opt. Exp. **26**, 15972 (2018).
[29] J. D. Benck, T. R. Hellstern, J. Kibsgaard, P. Chakthranont, and T. F. Jaramillo, ACS Catal. **4**, 3957 (2014).
[30] J. Baek, T. Umeyama, W. Choi, Y. Tsutsui, H. Yamada, S. Seki, and H. Imahori, Chem. Eur. J. **24**, 1561 (2017).
[31] D. Zeng, L. Xiao, W.-J. Ong, P. Wu, H. Zheng, Y. Chen, and D.-L. Peng, ChemSusChem **10**, 4624 (2017).
[32] For a review see for instance: E. Rahmanian, R. Malekfar, and M. Pumera, Chem. Eur. J. **24**, 18 (2017), and references therein.
[33] G. Deokar, P. Vancso, R. Arenal, F. Ravaux, J. Casanova-Chafer, E. Llobet, A. Makarova, D. Vyalikh, C. Struzzi, P. Lambin *et al.*, Adv. Mat. Int. **4**, 1700801 (2017); Y. Li, Y. L. Li, B. S. Sa, and R. Ahuja, Catalysis Sci. Techn. **7**, 545 (2017).
[34] For a review see for instance: G. Eda and S. A. Maier, ACS Nano **7**, 5660 (2013), and references therein.

[35] A. Splendiani, L. Sun, Y. Zhang, T. Li, J. Kim, C.-Y. Chim, G. Galli, and F. Wang, Nano Lett. **10**, 1271 (2010).

[36] E. Scalise, M. Houssa, G. Pourtois, V. Afanasév, and A. Stesmans, Nano Res. **5**, 43 (2012).

[37] P. Johari and V. B. Shenoy, ACS Nano **6**, 5449 (2012).

[38] P. Lu, X. Wu, W. Guo, and X. C. Zeng, Phys. Chem. Chem. Phys. **14**, 13035 (2012).

[39] W. S. Yun, S. W. Han, S. C. Hong, I. G. Kim, and J. D. Lee, Phys. Rev. B **85**, 033305 (2012).

[40] H. Peelaers and C. G. Van de Walle, Phys. Rev. B **86**, 241401 (2012).

[41] H. Shi, H. Pan, Y.-W. Zhang, and B. I. Yakobson, Phys. Rev. B **87**, 155304 (2013).

[42] S. Horzum, H. Sahin, S. Cahangirov, P. Cudazzo, A. Rubio, T. Serin, and F. M. Peeters, Phys. Rev. B **87**, 125415 (2013).

[43] M. Ghorbani-Asl, S. Borini, A. Kuc, and T. Heine, Phys. Rev. B **87**, 235434 (2013).

[44] Q. Zhang, Y. Cheng, L.-Y. Gan, and U. Schwingenschlögl, Phys. Rev. B **88**, 245447 (2013).

[45] E. Scalise, M. Houssa, G. Pourtois, V. Afanasév, and A. Stesmans, Physica E **56**, 416 (2014).

[46] D. M. Guzman and A. Strachan, J. Appl. Phys. **115**, 243701 (2014).

[47] L. Wang, A. Kutana, and B. I. Yakobson, Ann. Phys. **526**, L7 (2014).

[48] For a review see: R. Roldán, A. Castellanos-Gomez, E. Cappelluti, and F. Guinea, J. Phys.: Condens. Matter **27**, 313201 (2015).

[49] Y. Ye, X. Dou, K. Ding, D. Jiang, F. Yanga, and B. Sun, Nanoscale **8**, 10843 (2016).

[50] Y. Gong, Q. Zhou, X. Huang, B. Han, X. Fu, H. Gao, F. Li, and T. Cui, Chem. Nano Mat. **3**, 238 (2017).

[51] M. Peña-Álvarez, E. del Corro, Á. Morales-García, L. Kavan, M. Kalbac, and O. Frank, Nano Lett. **15**, 3139 (2015).

[52] Á. M. García, E. del Corro, M. Kalbacc, and O. Frank, Phys. Chem. Chem. Phys. **19**, 13333 (2017).

[53] P. Blaha, K. Schwarz, G. K. H. Madsen, D. Kvasnicka, and J. Luitz, *WIEN2K, An Augmented Plane Wave + Local Orbitals Program for Calculating Crystal Properties* (Karl-Heinz Schwarz, Techn. Universität, Wien, Austria, 2001).

[54] J. P. Perdew, K. Burke, and M. Ernzerhof, Phys. Rev. Lett. **77**, 3865 (1996).

[55] T. Brumme, M. Calandra, and F. Mauri, Phys. Rev. B **91**, 155436 (2015).

[56] R. Roldán, M. P. Lopéz-Sancho, F. Guinea, E. Cappelluti, J. A. Silva-Guillén, and P. Ordejón, 2D Mater. **1**, 034003 (2014).

[57] X. Zhang, X.-F. Qiao, W. Shi, J.-B. Wu, D.-S. Jiang, and P.-H. Tan, Chem. Soc. Rev. **44**, 2757 (2015).

[58] H. Tornatzky, R. Gillen, H. Uchiyama, and J. Maultzsch, arXiv:1809.03381.

[59] L. Boeri, E. Cappelluti, and L. Pietronero, Phys. Rev. B **71**, 012501 (2005).

[60] E. Cappelluti and L. Pietronero, J. Phys. Chem. Solids **67**, 1941 (2006).

[61] E. Cappelluti, R. Roldán, J. A. Silva-Guillén, P. Ordejón, and F. Guinea, Phys. Rev. B **88**, 075409 (2013).

[62] E. Cannuccia and A. Marini, Phys. Rev. Lett. **107**, 255501 (2011).

[63] E. Cannuccia and A. Marini, Eur. Phys. J. B **85**, 320 (2012).

[64] E. Cannuccia and A. Marini, arXiv:1304.0072.

[65] S. Poncé, G. Antonius, P. Boulanger, E. Cannuccia, A. Marini, M. Côté, and X. Gonze, Comput. Mat. Sci. **83**, 341 (2014).

[66] M. Cardona and M. L. W. Thewalt, Rev. Mod. Phys. **77**, 1173 (2005).

[67] P. B. Allen and V. Heine, J. Phys. C: Sol. State Phys. **9**, 2305 (1976).

[68] P. B. Allen and M. Cardona, Phys. Rev. B **23**, 1495 (1981).

[69] D. Y. Qiu, F. H. da Jornada, and S. G. Louie, Phys. Rev. Lett. **111**, 216805 (2013).

[70] D. Kozawa, R. Kumar, A. Carvalho, K. K. Amara, W. Zhao, S. Wang, M. Toh, R. M. Ribeiro, A. H. Castro Neto, K. Matsuda, and G. Eda, Nat. Commun. **5**, 4543 (2014).

[71] Y. Yu, Y. Yu, Y. Cai, W. Li, A. Gurarslan, H. Peelaers, D. E. Aspnes, C. G. Van de Walle, N. V. Nguyen, Y.-W. Zhang, and L. Cao, Sci. Rep. **5**, 16996 (2015).

[72] L. Wang, Z. Wang, H.-Y. Wang, G. Grinblat, Y. L. Huang, D. Wang, X.-H. Ye, X.-B. Li, Q. Bao, A.-S. Wee, S. A. Maier, Q.-D. Chen, M.-L. Zhong, C.-W. Qiu, and H.-B. Sun, Nat. Commun. **8**, 13906 (2017).

[73] W.-T. Hsu, Li-Syuan Lu, D. Wang, J.-K. Huang, M.-Y. Li, T.-R. Chang, Y.-C. Chou, Z.-Y. Juang, H.-T. Jeng, L.-J. Li, and W.-H. Chang, Nat. Commun. **8**, 929 (2017).

[74] J. T. Ye, Y. J. Zhang, R. Akashi, M. S. Bahramy, R. Arita, and Y. Iwasa, Science **338**, 1193 (2012).

[75] R. Roldán, E. Cappelluti, and F. Guinea, Phys. Rev. B **88**, 054515 (2013).

[76] J. M. Lu, O. Zheliuk, I. Leermakers, N. F. Q. Yuan, U. Zeitler, K. T. Law, and J. T. Ye, Science **350**, 1353 (2015).

[77] W. Shi, J. T. Ye, Y. Zhang, R. Suzuki, M. Yoshida, J. Miyazaki, N. Inoue, Y. Saito, and Y. Iwasa, Sci. Rep. **5**, 12534 (2015).

[78] S. Jo, D. Costanzo, H. Berger, and A. F. Morpurgo, Nano Lett. **15**, 1197 (2015).

[79] D. Costanzo, S. Jo, H. Berger, and A. F. Morpurgo, Nat. Nanotech. **11**, 339 (2016).

[80] Y. Saito, Y. Nakamura, M. S. Bahramy, Y. Kohama, J. T. Ye, Y. Kasahara, Y. Nakagawa, M. Onga, M. Tokunaga, T. Nojima, Y. Yanase, and Y. Iwasa, Nat. Phys. **12**, 144 (2016).